

# Metabolomics-Driven LC-HRMS Identification and Multi-Target Computational Pharmacology of *Shzygium polyanthum* Bioactives for Mechanism-Based Precision Management of Type 2 Diabetes Mellitus

Said Haikal Alfajar<sup>1</sup>, Urip Harahap<sup>2</sup>, Aminah Dalimunthe<sup>3</sup>, Nur Aira Juwita<sup>4</sup>,  
Rony Abdi Syahputra<sup>5</sup>

<sup>1,2,3,4,5</sup>Universitas Sumatera Utara, Medan, Indonesia

Email: [rony@usu.ac.id](mailto:rony@usu.ac.id)

## Abstract

Type 2 Diabetes Mellitus (T2DM) continues to be a major cause of mortality and metabolic complications in developing nations, highlighting the urgent need for safer and more accessible therapies. Herbal bioactives from *Syzygium polyanthum* (SYPOL) have gained attention due to their traditional use in managing blood glucose levels. Nevertheless, the molecular mechanisms underlying their antidiabetic effects remain poorly understood. This study employed an integrative in silico approach to evaluate the interactions between SYPOL-derived compounds and ten key protein targets involved in T2DM pathogenesis, including HK2, AKT1, PYGL, INSR, PYGM, IGF1R, PPARG, SLC2A1, MAPK3, and GCK. Ethanolic leaf extracts of SYPOL were analyzed using Liquid Chromatography–High Resolution Mass Spectrometry (LC-HRMS) for phytochemical profiling. Detected compounds were screened for structural availability, toxicity, ADME properties, and compliance with Lipinski's Rule of Five prior to molecular docking. From 9,834 detected phytochemical features, 31 compounds met the selection criteria and were docked against the ten diabetes-related targets. The simulations revealed stable interactions within active site regions, primarily driven by hydrogen bonding and favorable binding energies, suggesting potential modulation of glucose metabolism and insulin signaling pathways. ADME profiling indicated acceptable pharmacokinetic properties, with most compounds satisfying Lipinski's parameters. Toxicity prediction showed a 54.83% probability of nephrotoxicity, emphasizing the importance of safety validation in future studies SYPOL contains multi-target bioactive compounds with potential to regulate glucose homeostasis. This computational analysis provides a mechanistic basis for subsequent experimental research and supports the development of SYPOL-based phytotherapeutics for T2DM management.

**Keywords:** *Computational Pharmacology, Drug-Likeness, Enzyme Inhibitors, Herbal Medicine, Molecular Docking.*



## A. INTRODUCTION

The worldwide impact of degenerative conditions, with diabetes mellitus at the forefront, continues to intensify (Renzo et al., 2021). Lifestyle transformations, including urban expansion, elevated sugar intake, and physical inactivity, have accelerated this trajectory (Tseng et al., 2021). Sustained hyperglycemia not only defines the disease but also precipitates downstream complications such as cardiovascular events, renal dysfunction, and nerve damage, all of which elevate mortality risk (Renzo et al., 2021). Global statistics reveal that over 589 million adults currently contend with diabetes, a number expected to surpass 850 million shortly.

Mortality data from 2024 attributes approximately 3.4 million deaths among middle-aged adults to diabetic complications. Developing nations experience the heaviest toll, with Indonesia positioned among the highest-prevalence countries, 20.4 million current cases, projected to exceed 28 million by mid-century (IDF, 2025). These figures underscore the imperative for novel therapeutic approaches that are both effective and widely accessible. Standard T2DM treatments, including metformin, sulfonylureas, and  $\alpha$ -glucosidase inhibitors, achieve glycemic control but frequently induce adverse effects ranging from gastrointestinal distress to dangerous hypoglycemia, potentially undermining long-term compliance (Welz et al., 2018; Xie et al., 2023). This limitation has fueled investigation into alternative modalities with potentially superior safety profiles (Quinlan, 2022).

Herbal remedies, deeply embedded in ethnopharmacological traditions, remain integral to diabetes management across numerous developing regions (Pirintzos et al., 2022). Such approaches offer cultural resonance, economic feasibility, and alignment with conservation goals. Historical evidence demonstrates that traditional medicine systems have repeatedly provided blueprints for pharmaceutical innovation (Aware et al., 2022). *Syzygium polyanthum* has emerged as a species of particular interest. Its flowers have historically been prepared as infusions for blood sugar regulation (Jeyaraj et al., 2021), while leaf decoctions remain a common self-management strategy among T2DM patients (Ismail & Wan Ahmad, 2019; Widodo et al., 2024). Preclinical investigations by (Widyawati et al., 2023) corroborate these traditional applications, demonstrating measurable antihyperglycemic effects *in vivo*. Nevertheless, the mechanistic basis for these observations remains inadequately characterized.

The potential for SYPOL constituents to simultaneously engage multiple protein targets relevant to glucose homeostasis has not been thoroughly examined. T2DM's complex etiology—spanning insulin signaling defects, pancreatic dysfunction, and metabolic dysregulation—demands analytical frameworks capable of capturing such complexity. Computational strategies offer precisely this capability. Integration of metabolomic profiling with predictive algorithms and interaction analysis enables systematic exploration of compound-target networks.

The present study employs LC-HRMS for comprehensive phytochemical characterization of SYPOL leaves, followed by network pharmacology to elucidate interactions with glucose-regulatory proteins (Gharge et al., 2021). Through this integrative strategy, critical nodes within glucose homeostasis pathways are expected to be identified, and the multi-target mechanisms underlying the antidiabetic activity of SYPOL leaves are intended to be elucidated. By integrating advanced metabolomic profiling with computational systems biology, a data-driven foundation is established for rational phytopharmaceutical development, thereby contributing to the evolving paradigm of multi-target precision ethnopharmacology in the context of T2DM

## **B. EXPERIMENTAL SECTION**

### **1. Chemicals, Equipment, and Software**

All computational analyses were performed on an ASUS Vivobook® (AMD Ryzen 3, 8 GB RAM, Windows 11 Home 64-bit). Software included PyMOL v3.1.0 (RMSD analysis), PyRx v0.8 (AutoDock Vina engine for docking), Discovery Studio Visualizer 2024 (protein preparation and interaction analysis), and Cytoscape v3.10.3 with the CytoHubba plugin (network analysis). Laboratory equipment included a rotary evaporator (Heidolph®), LC-HRMS system (Thermo Scientific™), analytical balance, 0.20 µm nylon membrane filters, and refrigerated storage. Analytical-grade 96% ethanol and HPLC-grade methanol were used throughout.

### **2. Plant Authentication and Extraction**

Vouchered specimens (677/MEDA/2025) of fresh *Syzygium polyanthum* leaves from the Herbarium Medanense were used in this study. A 100 g portion was macerated with 1 L of 96% ethanol for 72 h at 2–8°C in the dark. Following maceration, the extract was filtered and concentrated under reduced pressure at 40 ± 1°C using a rotary evaporator, then stored at 2–8°C until analysis (Dewijanti et al., 2020).

### **3. LC-HRMS Phytochemical Profiling**

Sample preparation for LC-HRMS involved diluting 100 µL of extract with 900 µL of HPLC-grade methanol and filtering (0.20 µm). Analysis was performed on a Thermo Scientific™ LC-HRMS system, where compounds were tentatively identified using accurate mass and fragmentation patterns (Kusuma et al., 2025; Windarsih et al., 2022).

### **4. Compound Validation and Screening**

Compound validation involved cross-referencing with PubChem. Structures unavailable in PubChem were reconstructed using the RCSB PDB Chemical Sketch Tool and saved as SMILES. Classification with LIPID MAPS was used to retain only secondary metabolites. Subsequent toxicity screening with ProTox-3 selected compounds in classes 4–6, and their protein targets were predicted using SwissADME.

### **5. Target Identification and Network Analysis**

To identify potential targets, protein predictions from SwissADME were intersected with T2DM-related genes retrieved from GeneCards (relevance score ≥15) and OMIM. The overlapping targets, visualized via a Venn Diagram, were then used to construct a protein–protein interaction (PPI) network in STRING. This network, built with a high confidence score of 0.900 for *Homo sapiens*, was subsequently imported into Cytoscape for topological analysis. Using the CytoHubba plugin, the top 10 hub proteins were identified and prioritized for docking. Structural coordinates for these proteins were downloaded from the RCSB Protein Data Bank, ensuring each

met the quality criteria of a resolution  $<3 \text{ \AA}$ , X-ray diffraction determination, human origin, and no mutations.

## 6. Molecular Docking

Protein structures were prepared using Discovery Studio by removing water and heteroatoms and adding hydrogens. Redocking validation was performed by aligning the grid box to the native ligand; an RMSD  $<2.0 \text{ \AA}$  between the redocked and native poses confirmed the protocol's validity (Venkanna et al., 2020). Using PyRx v0.8, docking simulations were performed by centering the grid box on the active site and setting the exhaustiveness to 100. For each ligand, binding affinities (kcal/mol) and conformations were recorded. Subsequently, the highest-ranked poses were visually inspected to identify hydrogen bonds and other crucial interactions with surrounding residues (Chaudhary Kurmi & Karati, 2025).

## 7. Drug-Likeness, ADME, and Toxicity Prediction

Compliance with Lipinski's Rule of Five (Ro5)—specifically molecular weight  $<500 \text{ Da}$ , hydrogen bond acceptors  $<10$ , hydrogen bond donors  $<5$ , and  $\text{LogP} <5$ —was assessed using the PKCSM server (Ali et al., 2024). Subsequent ADME profiling, covering absorption, distribution, metabolism, and excretion, was also conducted via PKCSM (Olaokun & Zubair, 2023). A comprehensive toxicity evaluation was then carried out using ProTox-3 (Banerjee et al., 2024), encompassing hepatotoxicity, nephrotoxicity, neurotoxicity, cardiotoxicity, carcinogenicity, immunotoxicity, mutagenicity, and cytotoxicity.

## C. RESULTS AND DISCUSSION

### 1. Results of Active Compound Identification by LC-HRMS

Untargeted LC-HRMS analysis of SYPOL leaves detected 9.834 compounds within a 25-minute runtime, including  $\alpha$ -cadinene,  $\alpha$ -cubebene,  $\alpha$ -humulene,  $\alpha$ -pinene,  $\beta$ -pinene, (+)-linalool, copaene, farnesol, and squalene, with retention times ranging from 5.56 to 16.62 minutes (Fig 1). Previous GC-MS studies have also identified various terpenes in SYPOL leaves, including squalene,  $\alpha$ -pinene, linalool,  $\alpha$ -tocopherol, nerolidol, and valencene (Ismail & Wan Ahmad, 2019; Rahim et al., 2018; Widyawati et al., 2022). A distinctive characteristic of SYPOL leaves is their fragrant aroma, attributed to their essential oil content. This essential oil, a hallmark component, imparts a potent scent and constitutes the primary source of its bioactivity, making the leaves a culinary flavoring agent. The oil is highly volatile, with its characteristic aroma resulting from a complex mixture of monoterpenes and sesquiterpenes (Mahmoud Dogara, 2021).

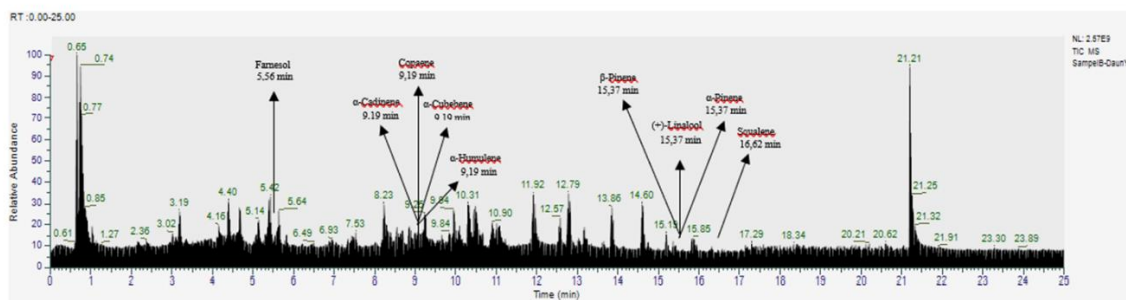


**Figure 1. Identification Results of Active Compounds of SYPOL leaves Using LC-MS.**

## 2. Results of Active Compound Screening for SYPOL Leaves

The marked reduction from thousands to a few dozen compounds illustrates a highly selective screening process. Consequently, only 0.33% of the bioactive compounds initially identified in SYPOL leaves satisfied all inclusion criteria and progressed for further analysis. This stringent filtration is detailed in Table 1.

**Table 1. Active Compounds of SYPOL Leaves**

| No. | Name                                                             | PubChem ID | Groups        | Prediction of Toxicity |
|-----|------------------------------------------------------------------|------------|---------------|------------------------|
| 1   | (+)-Linalool                                                     | 5281517    | Monoterpenes  | 5                      |
| 2   | 6-Hydroxyluteolin 6-xyloside                                     | 44258476   | Flavones      | 5                      |
| 3   | 9,10-Dihydro-10-(4-hydroxyphenyl)-pyrano(2,3-h)epicatechin-8-one | 44157102   | Flavonols     | 5                      |
| 4   | $\alpha$ -Pinene                                                 | 6654       | Monoterpenes  | 5                      |
| 5   | $\alpha$ -Cubebene                                               | 14869      | Sesquiterpene | 5                      |
| 6   | $\alpha$ -Curcumene                                              | 92139      | Sesquiterpene | 4                      |
| 7   | $\alpha$ -Humulene                                               | 5281520    | Sesquiterpene | 5                      |
| 8   | $\beta$ -Cadinene                                                | 10657      | Sesquiterpene | 5                      |
| 9   | $\beta$ -Pinene                                                  | 14896      | Monoterpenes  | 5                      |
| 10  | Adonixanthin                                                     | 16061189   | Tetraterpene  | 4                      |
| 11  | Capsorubin                                                       | 5281229    | Tetraterpene  | 5                      |
| 12  | Cerarvensin                                                      | 44257651   | Flavonols     | 4                      |
| 13  | Copaene                                                          | 12303902   | Sesquiterpene | 5                      |
| 14  | Echinonone                                                       | 5281236    | Tetraterpene  | 5                      |
| 15  | Farnesol                                                         | 445070     | Sesquiterpene | 4                      |
| 16  | Hovetrichoside C                                                 | 42607791   | Aurone        | 4                      |
| 17  | Kaempferol 7-neohesperidoside                                    | 5483905    | Flavonols     | 5                      |
| 18  | Kaempferol-3-O-glucoside-3''-rhamnoside                          | 74124649   | Flavonols     | 5                      |
| 19  | Linderoflavone A                                                 | 44258651   | Flavones      | 5                      |
| 20  | Luteolin 6-C-glucoside 8-C-arabinoside                           | 3549960    | Flavones      | 4                      |
| 21  | Maritimetin                                                      | 5281292    | Aurone        | 5                      |
| 22  | Melafolone                                                       | 5319329    | Chalcones     | 5                      |
| 23  | Morin                                                            | 5281670    | Flavones      | 5                      |
| 24  | Nothofagin                                                       | 21722188   | Chalcones     | 5                      |
| 25  | Okanin 4'- (6''-acetylglucoside)                                 | 42607561   | Chalcones     | 5                      |
| 26  | Quercetin-4'-glucoside                                           | 171380545  | Flavonols     | 5                      |
| 27  | Scutellarein                                                     | 5281697    | Flavones      | 5                      |
| 28  | Squalene                                                         | 638072     | Triterpenes   | 6                      |
| 29  | Taxifolin                                                        | 439533     | Flavanones    | 4                      |

|    |                             |         |               |   |
|----|-----------------------------|---------|---------------|---|
| 30 | Trans- $\beta$ -Damascenone | 5366074 | Tetraterpene  | 5 |
| 31 | Trans- $\beta$ -Farnesene   | 5281517 | Sesquiterpene | 4 |

The overlap between SYPOL leaf compounds and the GeneCards and OMIM databases yielded 568 potential target proteins. A subsequent PPI network analysis identified T2DM relevant targets, from which the top 10 hub proteins were selected using Cytoscape with its CytoHubba plugin. The complete selection workflow is depicted in Figure 2.

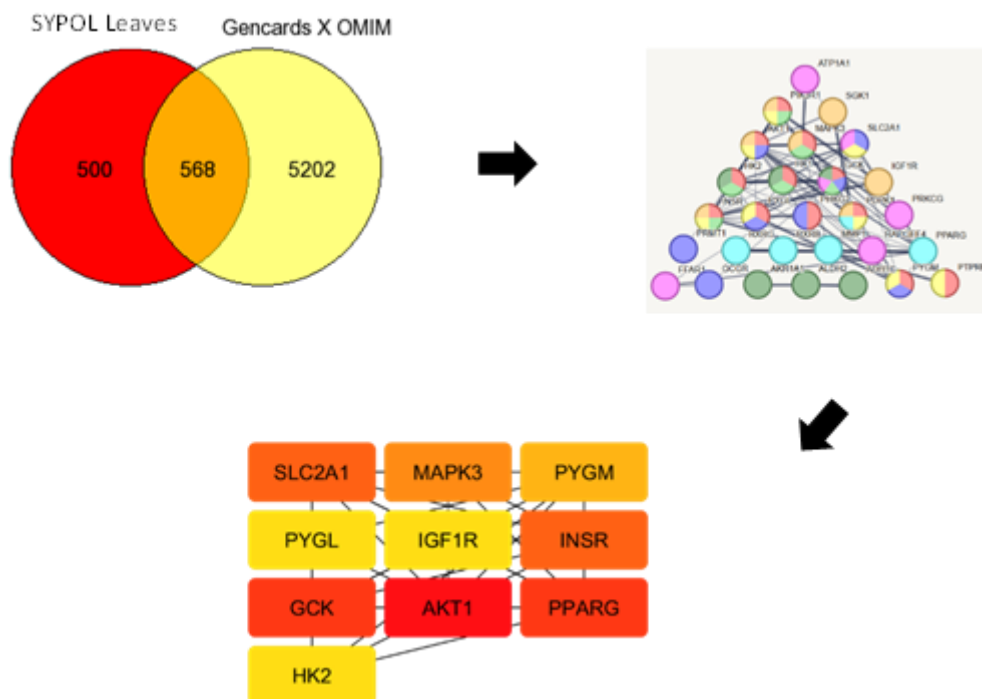


**Figure 2. Network Pharmacology Protein Target of SYPOL Leaves; (a) Overlapping Protein Targets; (b) Network Pharmacology of Protein Target; (c) Top 10 Protein Target Based on Genes**

Ten target proteins for SYPOL leaves were identified using Cytoscape with the 'Degree' ranking method. These targets were subsequently validated through redocking, confirming their suitability based on an acceptable RMSD threshold of < 2 Å (Table 2).

**Table 2. Target Proteins of SYPOL Leaves**

| No | Name | PDB ID | Resolution (Å) | Organism     | Method            | DR (%) | MFR (%) |
|----|------|--------|----------------|--------------|-------------------|--------|---------|
| 1  | HK2  | 2NZZ   | 2,45           | Homo sapiens | X-Ray Diffraction | 4      | 96      |
| 2  | AKT1 | 7NH5   | 1,90           | Homo sapiens | X-Ray Diffraction | 3      | 97      |
| 3  | PYGL | 3DDS   | 1,80           | Homo sapiens | X-Ray Diffraction | 2      | 98      |
| 4  | INSR | 5E1S   | 2,26           | Homo sapiens | X-Ray Diffraction | 2      | 98      |
| 5  | PYGM | 1Z8D   | 2,30           | Homo sapiens | X-Ray Diffraction | 4      | 96      |

|    |        |      |      |              |                      |   |    |
|----|--------|------|------|--------------|----------------------|---|----|
| 6  | IGF1R  | 5FXQ | 2,30 | Homo sapiens | X-Ray<br>Diffraction | 3 | 97 |
| 7  | PPARG  | 5YCN | 2,15 | Homo sapiens | X-Ray<br>Diffraction | 2 | 98 |
| 8  | SLC2A1 | 6THA | 2,40 | Homo sapiens | X-Ray<br>Diffraction | 3 | 97 |
| 9  | MAPK3  | 4QTB | 1,40 | Homo sapiens | X-Ray<br>Diffraction | 2 | 98 |
| 10 | GCK    | 5V4X | 2,08 | Homo sapiens | X-Ray<br>Diffraction | 3 | 97 |

### 3. Results of Docking Simulation

Simulations were performed between the active compounds from SYPOL leaves and the selected target proteins. The target proteins selected were HK2, AKT1, PYGL, INSR, PYGM, IGF1R, PPARG, SLC2A1, MAPK3 and GCK. The results of the docking simulations are presented in Tab 3. Several bioactive compounds have shown potential interactions with various protein targets through docking simulations. Kaempferol-3-O-rutinoside binds to AKT1 (-11.2 kcal/mol) and PYGL (-10.1 kcal/mol), supporting potential involvement in insulin signaling (Deogratias et al., 2022; Liu et al., 2025). (+)-Linalool interacts via alkyl interactions with residues ILE 48, ALA 69, LEU 173, and VAL 56 on MAPK3 (-13.8 kcal/mol), which plays a role in stabilizing the ligand-protein complex and has the potential to modulate kinase activity (Chen et al., 2022). Cerarvensin from SYPOL leaves binds to PPARG (-10.1 kcal/mol) through  $\pi$ -sulfur contact with MET 348 (Albanese et al., 2022) and pi-alkyl interaction with VAL 83 which may contribute to receptor conformational stabilization and transcriptional modulation (Reza et al., 2025). Okanin 4'-(6"-acetylglucoside) forms a hydrogen bond with THR 213 and a T-shaped interaction with MET 462 on GCK (-8.7 kcal/mol), potentially influencing enzyme activity through ligand orientation stabilization (Rinaldi et al., 2022; Thi et al., 2024). Quercetin-4'-glucoside (-9.3 kcal/mol) forms a hydrogen bond with ASP 1150, which may enhance binding affinity to the receptor (Thi et al., 2024). Adonixanthin forms pi-alkyl contacts with LYS 191 and HIS 57, contributing to ligand-protein complex stabilization (Reza et al., 2025). 9,10-Dihydro-10-(4-hydroxyphenyl)-pyrano(2,3-h)epicatechin-8-one exhibits a donor-donor interaction with ARG 242 on PYGM (-9.4 kcal/mol), which may support isoform selectivity among glycogen phosphorylases (Irannejad et al., 2020), as well as a  $\pi$ -sigma interaction with a MET residue on IGF1R that may help maintain functional ligand orientation within the binding site (Irham et al., 2025). Collectively, these non-covalent interactions contribute to complex stabilization, enhanced affinity, and potential modulation of protein target activity.

SYPOL-derived metabolites exhibit a broad but modest affinity for multiple targets, suggesting multi-target modulation rather than potent single-pathway inhibition—a profile that aligns with the interconnected nature of T2DM pathophysiology, including insulin signaling, glycogen metabolism, and transcriptional regulation. However, molecular docking only predicts structural

compatibility, not biological activity. Key factors such as bioavailability, metabolic transformation (e.g., deglycosylation or conjugation of glycosylated flavonoids), enzyme kinetics, and cellular permeability remain unexamined. Although SYPOL leaves are traditionally used for glycemic control, concurrent use with standard antidiabetic drugs without medical supervision may pose risks of pharmacodynamic interaction (Moaberfard, 2019). Thus, *in vitro*, cellular, and *in vivo* studies are necessary to validate these *in silico* findings. LC-HRMS enabled the identification of specific active compounds, which were further analyzed via docking simulations. These simulations predicted binding interactions—including covalent bonds—with target proteins, offering structural insights into potential functional mechanisms (Khan et al., 2018). While previous studies have reported the blood glucose-lowering (BGL) effects of SYPOL leaves (Parisa et al., 2019; Widodo et al., 2024; Widyawati et al., 2022), they did not specifically investigate isolated compounds such as cerarvensin. Hence, further research is needed to confirm the efficacy of SYPOL leaves in reducing BGL through compound-specific approaches.

**Table 3. Results of Docking Simulation for Active Compounds from SYPOL Leaves**

| Protein Targets | Compounds                                                        | Binding affinity (kcal/mol) | Hydrogen Bond                                                                                                      |
|-----------------|------------------------------------------------------------------|-----------------------------|--------------------------------------------------------------------------------------------------------------------|
| PYGM            | 9,10-Dihydro-10-(4-hydroxyphenyl)-pyrano(2,3-h)epicatechin-8-one | -9,4                        | GLY 317, PHE 196, ARG 242, ARG 309, TYR 75, ARG 319                                                                |
| IGF1R           | 9,10-Dihydro-10-(4-hydroxyphenyl)-pyrano(2,3-h)epicatechin-8-one | -7,8                        | LEU 1005, ALA 1031, VAL 1013, ASP 1153, MET 1142                                                                   |
| PPARG           | Cerarvensin                                                      | -10,1                       | VAL 83, SER 80, THR 137, TRP 388, GLN 282                                                                          |
| SLC2A1          | Cerarvensin                                                      | -10,1                       | VAL 83, SER 80, THR 137, TRP 388, GLN 282                                                                          |
| MAPK3           | (+)-Linalool                                                     | -13,8                       | TYR 81, ALA 52, ARG 84, TYR 53, ILE 73, LYS 71, LYS 131, ILE 48, MET 125, ASP 123, ALA 69, VAL 56, LEU 173, LYS 71 |
| GCK             | Okanin 4'- (6"-acetylglucoside)                                  | -8,7                        | MET 462, VAL 455, LYS 458, VAL 62, TYR 214, SER 64, ARG 63, PRO 66, TRP 99, TYR 61                                 |
| HK2             | Okanin 4'- (6"-acetylglucoside)                                  | -9,5                        | THR 232, THR 88, SER 415, THR 213, ASP 209, SER 155, ASP 84, SER 449, LYS 418                                      |
| AKT1            | Kaempferol-3-O-glucoside-3"-rhamnoside                           | -11,2                       | LEU 210, ASN 204, TRP 80, LEU 264, VAL 270, LYS 268, GLN 79, ASP 292, ASN 53                                       |
| PYGL            | Adonixanthin                                                     | -9,8                        | GLU 1162, LYS 191, HIS 57, HIS 34, ARG 33, HIS 34                                                                  |

|      |                        |      |                                                                                      |
|------|------------------------|------|--------------------------------------------------------------------------------------|
| INSR | Quercetin-4'-glucoside | -9,3 | HIS 1081, ALA 1080, LEU 1002,<br>MET 1079, ALA 1028, MET 1139,<br>ASP 1150, VAL 1010 |
|------|------------------------|------|--------------------------------------------------------------------------------------|

The docking results of the active compound against the protein target are provided in the supplementary files.

#### 4. Results of Ro5 Prediction for Active Compounds of SYPOL Leaves

Ro5 compliance was assessed for 31 bioactive compounds from SYPOL leaves (Table 4). Among these, luteolin 6-C-glucoside 8-C-arabinoside exhibited the highest molecular weight at 610.521 Dalton.

**Table 4. Ro5 of Active Compounds from SYPOL Leaves**

| No | Compounds                                                        | Ro5     |     |     |          |
|----|------------------------------------------------------------------|---------|-----|-----|----------|
|    |                                                                  | MW      | HBA | HBD | Log P    |
| 1  | (+)-Linalool                                                     | 154,253 | 1   | 1   | 2,6698   |
| 2  | 6-Hydroxyluteolin 6-xyloside                                     | 434,353 | 11  | 7   | 0,1002   |
| 3  | 9,10-Dihydro-10-(4-hydroxyphenyl)-pyrano(2,3-h)epicatechin-8-one | 436,416 | 8   | 5   | 2,9871   |
| 4  | $\alpha$ -Pinene                                                 | 136,238 | 0   | 0   | 2,9987   |
| 5  | $\alpha$ -Cubebene                                               | 204,357 | 0   | 0   | 4,2709   |
| 6  | $\alpha$ -Curcumene                                              | 202,341 | 0   | 0   | 4,84492  |
| 7  | $\alpha$ -Humulene                                               | 204,357 | 0   | 0   | 5,0354   |
| 8  | $\beta$ -Cadinene                                                | 204,357 | 0   | 0   | 4,5811   |
| 9  | $\beta$ -Pinene                                                  | 136,238 | 0   | 0   | 2,9987   |
| 10 | Adonixanthin                                                     | 582,869 | 3   | 2   | 9,7264   |
| 11 | Capsorubin                                                       | 600,884 | 4   | 2   | 9,0652   |
| 12 | Cerarvensin                                                      | 550,871 | 1   | 0   | 11,7848  |
| 13 | Copaene                                                          | 204,357 | 0   | 0   | 4,2709   |
| 14 | Echinenone                                                       | 550,871 | 1   | 0   | 11,7848  |
| 15 | Farnesol                                                         | 222,372 | 1   | 1   | 4,3979   |
| 16 | Hovetrichoside C                                                 | 450,396 | 11  | 7   | -1,12171 |
| 17 | Kaempferol 7-neohesperidoside                                    | 594,522 | 15  | 9   | -1,3927  |
| 18 | Kaempferol-3-O-glucoside-3''-rhamnoside                          | 594,522 | 15  | 9   | -1,3927  |
| 19 | Linderoflavone A                                                 | 358,302 | 8   | 2   | 2,6171   |
| 20 | Luteolin 6-C-glucoside 8-C-arabinoside                           | 610,521 | 16  | 12  | -2,6878  |
| 21 | Maritimetin                                                      | 370,313 | 8   | 0   | 2,9346   |
| 22 | Melafolone                                                       | 400,427 | 7   | 2   | 3,9626   |
| 23 | Morin                                                            | 302,238 | 7   | 5   | 1,988    |
| 24 | Nothofagin                                                       | 436,413 | 10  | 8   | -0,1606  |
| 25 | Okanin 4'-(6''-acetylglucoside)                                  | 492,433 | 12  | 7   | 0,1546   |
| 26 | Quercetin-4'-glucoside                                           | 464,379 | 12  | 8   | -0,5389  |
| 27 | Scutellarein                                                     | 286,239 | 6   | 4   | 2,2824   |
| 28 | Squalene                                                         | 410,73  | 0   | 0   | 10,605   |
| 29 | Taxifolin                                                        | 304,254 | 7   | 5   | 1,1863   |
| 30 | Trans- $\beta$ -damascenone                                      | 190,286 | 1   | 0   | 3,4342   |
| 31 | Trans- $\beta$ -Farnesene                                        | 204,357 | 0   | 0   | 5,2015   |

The Ro5, introduced by Christopher A. Lipinski in 1997, remains a fundamental guideline in drug design for predicting the oral bioavailability of small molecules based on their physicochemical properties (Zheng et al., 2025). It is widely regarded as the most relevant and accurate screening tool for this purpose (Ojuka et al., 2023). The rule is named for its key numerical thresholds—molecular weight <500 Da, Log P <5, hydrogen bond donors <5, and hydrogen bond acceptors <10—all of which are multiples of five (Ali et al., 2024; Pollastri, 2010).

These criteria serve as an initial filter: molecular weight under 500 Da facilitates membrane permeability, Log P below 5 ensures optimal lipophilicity, and limited hydrogen bond donors and acceptors prevent impaired lipid membrane penetration (Ali et al., 2024). Compounds satisfying all four Ro5 criteria are more likely to exhibit good oral bioavailability and be efficiently absorbed through the gastrointestinal tract to reach their biological targets (Ashraf et al., 2021). Copaene compounds isolated from SYPOL leaves meet all Ro5 requirements, including molecular weight, Log P, hydrogen bond donors, and hydrogen bond acceptors. Therefore, they are predicted to be promising novel candidates for alternative T2DM therapy. However, comprehensive follow-up research utilizing *in vitro* and *in vivo* approaches remains essential to thoroughly analyze their safety and efficacy profiles before therapeutic application can be considered.

## 5. Prediction of Pharmacokinetic Properties for Active Compounds from SYPOL Leaves

This study evaluated the ADME properties of active compounds from SYPOL leaves to assess their pharmacokinetic potential (Tab 5). In terms of absorption, linderoflavone A exhibited high absorption (98.669%) (Rhabori et al., 2025), which is favorable for ensuring sufficient compound reaches systemic circulation. Cerarvensin demonstrated sparingly soluble properties with a log S value of 7.274 mol/L (Sanober & Agarwal, 2021), indicating limited aqueous solubility that may affect dissolution.  $\alpha$ -Curcumene showed moderate Caco-2 permeability ( $1.537 \times 10^{-6}$  cm/s) (Kus et al., 2023), suggesting reasonable intestinal absorption capacity. Regarding distribution, 6-Hydroxyluteolin 6-xyloside exhibited high tissue distribution (VD<sub>ss</sub> 1.851 log L/kg) (Silva et al., 2023), indicating good ability to reach extravascular targets, while cerarvensin heptapeptide remained largely confined to plasma (VD<sub>ss</sub> 0.035 log L/kg) (Silva et al., 2023), which may limit tissue penetration. For plasma protein binding, (+)-linalool showed low binding (FU 48.4%) (Ma et al., 2021), meaning a larger free fraction is pharmacologically available, whereas linderoflavone A exhibited high binding (FU 0.1%) (Ma et al., 2021), potentially reducing free drug concentration. In metabolism evaluation,  $\alpha$ -Cubebene was identified as a CYP1A2 inhibitor (Zhao et al., 2021), which could affect co-administered drug metabolism, and none of the compounds were substrates for OCT2 (Noorlander et al., 2023), suggesting a favorable safety profile for patients with renal impairment. Collectively, favorable ADME parameters—such as high absorption, optimal distribution, appropriate protein binding, and minimal drug interaction liability—enhance the likelihood of a

compound achieving therapeutic concentrations at target sites with reduced toxicity risk, supporting further development of SYPOL-derived compounds as potential therapeutic agents (Verma et al., 2025).

**Table 5. ADME Prediction for Active Compounds of SYPOL Leaves**

| Compound                                                         | Absorption                   |                                            |               | Distribution                    |                         |                           |                  |                 | Metabolism       |                       |                           |                           |                          | Excretion                  |                          |                           |                          |                                       |                      |
|------------------------------------------------------------------|------------------------------|--------------------------------------------|---------------|---------------------------------|-------------------------|---------------------------|------------------|-----------------|------------------|-----------------------|---------------------------|---------------------------|--------------------------|----------------------------|--------------------------|---------------------------|--------------------------|---------------------------------------|----------------------|
|                                                                  | Water solubility (Log mol/L) | Caco2 permeability (10 <sup>-6</sup> cm/s) | GI absorption | Skin permeability log Kp (Cm/s) | P-gp substrate (Yes/No) | P-gp I inhibitor (Yes/No) | P-gp II (Yes/No) | VDss (log L/kg) | Fraction unbound | BBB permeant (Log BB) | CNS permeability (Log Ps) | CYP3A4 substrate (Yes/No) | CYP1A2 inhibitor(Yes/No) | CYP2C19 inhibitor (Yes/No) | CYP2C9 inhibitor(Yes/No) | CYP2D6 inhibitor (Yes/No) | CYP3A4 inhibitor(Yes/No) | Total renal clearance (Log ml/min/kg) | Renal OCT2 Substrate |
| (+)-Linalool                                                     | 2.612                        | 1.493                                      | 93.163        | 1.737                           | No                      | No                        | No               | 0.152           | 0.484            | 0.598                 | -2.339                    | No                        | No                       | No                         | No                       | No                        | No                       | 0.446                                 | No                   |
| 6-Hydroxyluteolin                                                | 2.906                        | 0.199                                      | 48.162        | 2.735                           | Yes                     | No                        | No               | 1.851           | 0.137            | -1.673                | -4.212                    | No                        | No                       | No                         | No                       | No                        | No                       | 0.037                                 | No                   |
| 6-xyloside                                                       | -                            | -                                          | -             | -                               | Yes                     | Yes                       | Yes              | -               | 0.001            | -                     | -                         | Yes                       | No                       | No                         | No                       | No                        | Yes                      | 0.136                                 | No                   |
| 9,10-Dihydro-10-(4-hydroxyphenyl)-pyrano(2,3-h)epicatechin-8-one | 3.118                        | 0.154                                      | 78.186        | 2.735                           | Yes                     | Yes                       | Yes              | 0.0439          | 0.001            | -1.373                | -3.367                    | No                        | No                       | No                         | No                       | No                        | Yes                      | 0.136                                 | No                   |
| α-Pinene                                                         | 3.733                        | 1.38                                       | 96.041        | 1.827                           | No                      | No                        | No               | 0.667           | 0.425            | 0.791                 | -2.201                    | No                        | No                       | No                         | No                       | No                        | No                       | 0.043                                 | No                   |
| α-Cubebene                                                       | 5.968                        | 1.389                                      | 95.964        | 1.997                           | No                      | No                        | No               | 0.077           | 0.114            | 0.86                  | 1.552                     | No                        | Yes                      | No                         | No                       | No                        | No                       | 0.98                                  | No                   |
| α-curcume                                                        | 5.962                        | 1.537                                      | 93.29         | 1.477                           | No                      | No                        | No               | 1.089           | 0.015            | 0.593                 | -1.554                    | No                        | Yes                      | No                         | No                       | No                        | No                       | 1.511                                 | No                   |
| α-Humule                                                         | 5.191                        | 1.421                                      | 94.682        | 1.739                           | Yes                     | No                        | No               | 0.055           | 0.037            | 0.663                 | -2.555                    | No                        | No                       | No                         | No                       | No                        | No                       | 1.282                                 | No                   |
| β-Cadinene                                                       | 5.816                        | 1.434                                      | 97.155        | 1.481                           | No                      | No                        | No               | 0.069           | 0.199            | 0.789                 | -1.955                    | No                        | No                       | No                         | No                       | No                        | No                       | 1.177                                 | No                   |

|                                        |                    |               |                 |                    |             |             |             |                    |               |                |                |    |     |     |     |        |        |             |               |        |
|----------------------------------------|--------------------|---------------|-----------------|--------------------|-------------|-------------|-------------|--------------------|---------------|----------------|----------------|----|-----|-----|-----|--------|--------|-------------|---------------|--------|
| β-Pinene                               | -<br>4,<br>19<br>1 | 1,<br>38<br>5 | 95,<br>525      | -<br>1,<br>65<br>3 | N<br>o      | N<br>o      | N<br>o      | 0,<br>68<br>5      | 0,<br>35      | 0,81<br>8      | -<br>1,85<br>7 | No | No  | No  | No  | N<br>o | N<br>o | N<br>o      | 0,<br>03      | N<br>o |
| Adonixanthin                           | -<br>6,<br>63<br>4 | 1,<br>23<br>9 | 90,<br>741      | -<br>2,<br>73<br>8 | Y<br>e<br>s | N<br>o      | Y<br>e<br>s | -<br>0,<br>50<br>4 | 0             | 0,53<br>1      | -<br>1,18<br>7 | No | Yes | No  | No  | N<br>o | N<br>o | N<br>o      | 0,<br>88<br>1 | N<br>o |
| Capsorubin                             | -<br>6,<br>33<br>6 | 0,<br>42      | 91,<br>047      | -<br>2,<br>76<br>5 | N<br>o      | N<br>o      | Y<br>e<br>s | 0,<br>75<br>2      | 0             | 0,09<br>4      | -<br>1,66<br>4 | No | Yes | No  | No  | N<br>o | N<br>o | N<br>o      | 0,<br>95<br>7 | N<br>o |
| Cerarvensin                            | -<br>7,<br>27<br>4 | 1,<br>24<br>3 | 93,<br>0,7<br>7 | -<br>2,<br>73<br>8 | N<br>o      | N<br>o      | Y<br>e<br>s | 0,<br>03<br>5      | 0             | 0,79<br>7      | -<br>1,19<br>2 | No | Yes | No  | No  | N<br>o | N<br>o | N<br>o      | 0,<br>89<br>1 | N<br>o |
| Copaene                                | -<br>5,<br>70<br>5 | 1,<br>37<br>4 | 96,<br>221      | -<br>2,<br>22<br>5 | N<br>o      | N<br>o      | N<br>o      | 0,<br>80<br>6      | 0,<br>11<br>5 | 0,88<br>7      | -<br>1,65<br>9 | No | Yes | No  | No  | N<br>o | N<br>o | N<br>o      | 0,<br>95      | N<br>o |
| Echinene                               | -<br>7,<br>27<br>4 | 1,<br>24<br>3 | 93,<br>077      | -<br>2,<br>73<br>8 | N<br>o      | N<br>o      | Y<br>e<br>s | 0,<br>03<br>5      | 0             | 0,79<br>7      | -<br>1,19<br>2 | No | Yes | No  | No  | N<br>o | N<br>o | N<br>o      | 0,<br>89<br>1 | N<br>o |
| Farnesol                               | -<br>5,<br>39<br>3 | 1,<br>49<br>5 | 91,<br>531      | -<br>1,<br>51<br>4 | N<br>o      | N<br>o      | N<br>o      | 0,<br>36           | 0,<br>20<br>6 | 0,66           | -<br>1,93<br>3 | No | Yes | No  | No  | N<br>o | N<br>o | N<br>o      | 1,<br>75<br>4 | N<br>o |
| Hovetricoside C                        | -<br>2,<br>49<br>6 | 0,<br>45<br>8 | 41,<br>248      | -<br>2,<br>73<br>5 | Y<br>e<br>s | N<br>o      | N<br>o      | 0,<br>77<br>3      | 0,<br>27<br>1 | -<br>1,09<br>3 | -<br>4,15<br>7 | No | Yes | No  | No  | N<br>o | N<br>o | N<br>o      | 0,<br>07<br>1 | N<br>o |
| Kaempferol 7-neohesperidoside          | -<br>2,<br>9       | 1,<br>06<br>9 | 19,<br>578      | -<br>2,<br>73<br>5 | Y<br>e<br>s | N<br>o      | N<br>o      | 1,<br>29<br>3      | 0,<br>16<br>1 | -<br>1,80<br>7 | -<br>4,99<br>9 | No | Yes | No  | No  | N<br>o | N<br>o | N<br>o      | 0,<br>16<br>6 | N<br>o |
| Kaempferol-3-O-glucoside-3"-rhamnoside | -<br>2,<br>90<br>2 | 0,<br>47<br>8 | 30,<br>203      | -<br>2,<br>73<br>5 | Y<br>e<br>s | N<br>o      | N<br>o      | 0,<br>07<br>4      | 0,<br>21<br>3 | -<br>1,93<br>2 | -<br>5,60<br>4 | No | Yes | No  | No  | N<br>o | N<br>o | N<br>o      | 0,<br>06      | N<br>o |
| Linderoflavone A                       | -<br>3,<br>23<br>9 | 0,<br>47<br>1 | 98,<br>669      | -<br>2,<br>74<br>2 | Y<br>e<br>s | N<br>o      | Y<br>e<br>s | -<br>0,<br>15<br>6 | 0,<br>00<br>1 | -<br>0,81<br>2 | -<br>3,39<br>3 | No | Yes | No  | No  | N<br>o | N<br>o | Y<br>e<br>s | 0,<br>46<br>2 | N<br>o |
| Luteolin 6-C-glucoside 8-C-arabinoside | -<br>2,<br>88<br>1 | 1,<br>40<br>2 | 11,<br>639      | -<br>2,<br>73<br>5 | Y<br>e<br>s | N<br>o      | N<br>o      | 0,<br>73<br>3      | 0,<br>26<br>9 | -<br>2,11<br>4 | -<br>4,95<br>7 | No | Yes | No  | No  | N<br>o | N<br>o | N<br>o      | 0,<br>33<br>3 | N<br>o |
| Maritimetin                            | -<br>3,<br>86<br>4 | 1,<br>23<br>3 | 98,<br>116      | -<br>2,<br>74<br>2 | N<br>o      | Y<br>e<br>s | Y<br>e<br>s | -<br>0,<br>44<br>5 | 0,<br>12<br>3 | -<br>1,11<br>5 | -<br>3,38      | No | Yes | No  | No  | N<br>o | N<br>o | N<br>o      | 0,<br>35<br>6 | N<br>o |
| Melafolone                             | -<br>4,<br>51<br>5 | 0,<br>12<br>5 | 84,<br>526      | -<br>2,<br>75<br>4 | Y<br>e<br>s | Y<br>e<br>s | Y<br>e<br>s | 0,<br>12<br>4      | 0             | -<br>0,48<br>7 | -<br>2,97<br>4 | No | Yes | Yes | Yes | N<br>o | N<br>o | Y<br>e<br>s | 0,<br>18<br>8 | N<br>o |
| Morin                                  | -<br>2,<br>97<br>8 | 0,<br>29<br>4 | 75,<br>408      | -<br>2,<br>73<br>5 | Y<br>e<br>s | N<br>o      | N<br>o      | 1,<br>22<br>9      | 0,<br>21<br>4 | -<br>1,18      | -<br>3,38<br>9 | No | Yes | No  | No  | N<br>o | N<br>o | N<br>o      | 0,<br>48<br>6 | N<br>o |

|                                            |                    |                    |            |                    |             |             |             |                    |               |                |                |    |             |     |    |             |        |        |                    |        |
|--------------------------------------------|--------------------|--------------------|------------|--------------------|-------------|-------------|-------------|--------------------|---------------|----------------|----------------|----|-------------|-----|----|-------------|--------|--------|--------------------|--------|
| Nothofagin                                 | -<br>2,<br>81<br>7 | 0,<br>93<br>3      | 46,<br>385 | -<br>2,<br>73<br>5 | Y<br>e<br>s | N<br>o      | N<br>o      | 1,<br>22<br>6      | 0,<br>31<br>4 | -<br>1,33<br>4 | -<br>3,98<br>2 | No | N<br>o      | No  | No | N<br>o      | N<br>o | N<br>o | -<br>0,<br>07<br>1 | N<br>o |
| Okanin<br>4'- (6"-<br>acetylglu<br>coside) | -<br>2,<br>96<br>5 | -<br>0,<br>10<br>5 | 44,<br>408 | -<br>2,<br>73<br>5 | Y<br>e<br>s | Y<br>e<br>s | N<br>o      | 2,<br>11<br>9      | 0,<br>19<br>8 | -<br>1,83<br>1 | -<br>4,18<br>3 | No | N<br>o      | No  | No | N<br>o      | N<br>o | N<br>o | -<br>0,<br>01<br>8 | N<br>o |
| Querceti<br>n-4'-<br>glucosid<br>e         | -<br>2,<br>90<br>8 | -<br>2,<br>74      | 35,<br>947 | -<br>2,<br>73<br>5 | Y<br>e<br>s | N<br>o      | N<br>o      | 1,<br>99<br>9      | 0,<br>25<br>2 | -<br>1,69<br>8 | -<br>4,10<br>4 | No | N<br>o      | No  | No | N<br>o      | N<br>o | N<br>o | 0,<br>38           | N<br>o |
| Scutellar<br>ein                           | -<br>3,<br>06<br>3 | 0,<br>93<br>6      | 70,<br>092 | -<br>2,<br>73<br>6 | Y<br>e<br>s | N<br>o      | N<br>o      | -<br>0,<br>04<br>6 | 0,<br>11<br>1 | -<br>1,26<br>7 | -<br>2,48<br>8 | No | N<br>o      | Yes | No | Y<br>e<br>s | N<br>o | N<br>o | 0,<br>62<br>5      | N<br>o |
| Squalene                                   | -<br>8,<br>40<br>1 | 1,<br>19<br>3      | 89,<br>002 | -<br>2,<br>76<br>3 | N<br>o      | N<br>o      | Y<br>e<br>s | 0,<br>35           | 0             | 0,96<br>5      | -<br>0,93<br>5 | No | Y<br>e<br>s | No  | No | N<br>o      | N<br>o | N<br>o | 1,<br>79<br>1      | N<br>o |
| Taxifolin                                  | -<br>3,<br>04<br>2 | 0,<br>92<br>4      | 64,<br>709 | -<br>2,<br>73<br>5 | Y<br>e<br>s | N<br>o      | N<br>o      | 1,<br>63<br>8      | 0,<br>32      | -<br>0,72<br>5 | -<br>3,19<br>8 | No | N<br>o      | No  | No | N<br>o      | N<br>o | N<br>o | -<br>0,<br>07<br>8 | N<br>o |
| Trans- $\beta$ -<br>damasce<br>none        | -<br>3,<br>50<br>5 | 1,<br>22<br>9      | 96,<br>897 | -<br>1,<br>80<br>3 | N<br>o      | N<br>o      | N<br>o      | 0,<br>26<br>5      | 0,<br>40<br>2 | 0,60<br>4      | -<br>2,34<br>5 | No | N<br>o      | No  | No | N<br>o      | N<br>o | N<br>o | 0,<br>26<br>5      | N<br>o |
| Trans- $\beta$ -<br>Farnesen<br>e          | -<br>6,<br>95<br>6 | 1,<br>40<br>5      | 93,<br>432 | -<br>1,<br>28<br>1 | N<br>o      | N<br>o      | N<br>o      | 0,<br>57<br>4      | 0,<br>14<br>9 | 0,83<br>5      | -<br>1,66<br>9 | No | N<br>o      | No  | No | N<br>o      | N<br>o | N<br>o | 1,<br>83<br>2      | N<br>o |

## 6. Results of Toxicity Prediction for Active Compounds of SYPOL Leaves

Nephrotoxicity refers to kidney damage caused by exposure to heavy metals, medications, or specific chemical compounds. The kidneys function to filter the blood, allowing harmful substances to be excreted in urine (Kwiatkowska et al., 2021). However, continuous exposure can damage renal structures such as the glomeruli. This results in a decreased glomerular filtration rate, potentially leading to acute or chronic kidney failure. Common symptoms of nephrotoxicity include sepsis, DM and hypertension (Džidić-Krivić et al., 2024).

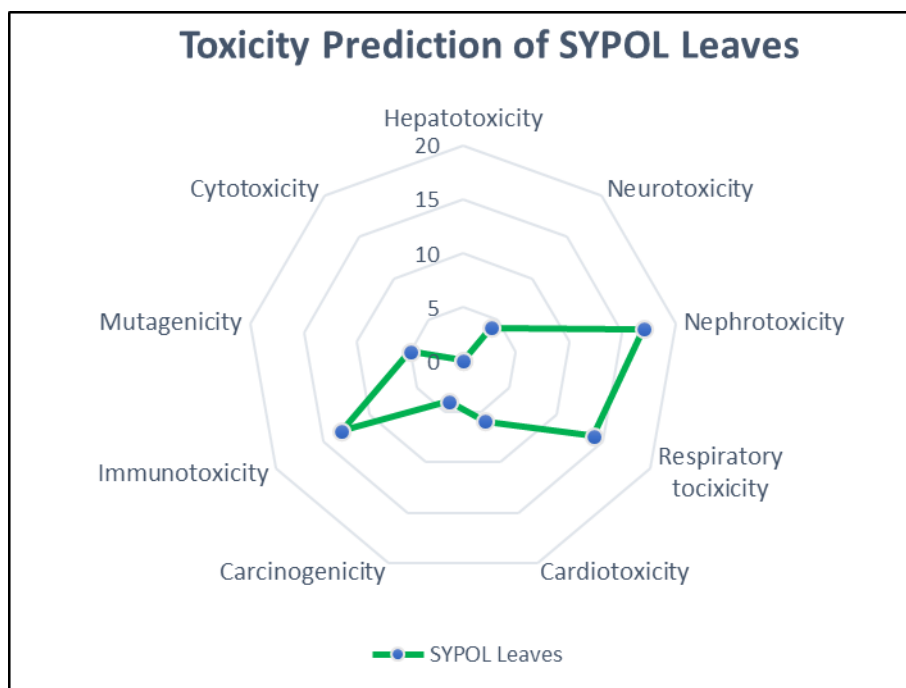


**Figure 3. Toxicity Prediction for Active Compounds of SYPOL Leaves**

Predictions from SwissaADME regarding the respiratory toxicity of SYPOL leaves compounds should be interpreted cautiously due to methodological limitations. The tool's accuracy may be limited, especially for complex natural products with unusual properties, posing a risk of errors. Variability in predictive power, lack of algorithm customization, and a focus on single-compound evaluation reduce its relevance for assessing toxicity in herbal mixtures. Moreover, SwissaADME does not offer detailed mechanistic insights into toxicity predictions, so findings should not be considered conclusive without further experimental validation (Nizamuddin et al., 2024). Predicting the toxicity of natural products is essential to ensure safety, reduce research costs and time, and thereby improve drug development efficiency. However, further studies are necessary to conclusively verify the safety of any natural material. *In vitro* and *in vivo* approaches are commonly employed to assess the toxic potential of compounds.

#### D. CONCLUSIONS

T2DM continues to be a major health concern, especially in developing nations. This research identified the phytochemical constituents of SYPOL using LC-HRMS and assessed their potential antidiabetic effects through an integrated *in silico* approach. A range of metabolites exhibited moderate to strong predicted binding affinities to key proteins involved in glucose regulation—such as HK2, AKT1, PYGL, INSR, PYGM, IGF1R, PPARG, SLC2A1, MAPK3, and GCK—indicating a possible multi-target mechanism of action. Although most compounds satisfied Lipinski's Rule of Five, only a few displayed favorable pharmacokinetic properties, and toxicity predictions suggested a potential risk of nephrotoxicity. These results offer an initial mechanistic insight into SYPOL's antidiabetic potential, but further experimental

confirmation through in vitro and in vivo studies is required to confirm its therapeutic applicability.

## REFERENCES

1. Albanese, K. I., Leaver-Fay, A., Treacy, J. W., Park, R., Houk, K. N., Kuhlman, B., & Waters, M. L. (2022). Comparative Analysis of Sulfonium- $\pi$ , Ammonium- $\pi$ , and Sulfur- $\pi$  Interactions and Relevance to SAM-Dependent Methyltransferases. *Journal of the American Chemical Society*, 144, 2535–2545. <https://doi.org/10.1021/jacs.1c09902>
2. Ali, M., Hassan, M., Ansari, S. A., Alkahtani, H. M., Al-Rasheed, L. S., & Ansari, S. A. (2024). Quercetin and Kaempferol as Multi-Targeting Antidiabetic Agents against Mouse Model of Chemically Induced Type 2 Diabetes. *Pharmaceuticals*, 17(6), 1–20. <https://doi.org/10.3390/ph17060757>
3. Ashraf, S. A., Elkhalfifa, A. E. O., Mehmood, K., & Adnan, M. (2021). Acid Targeting Signaling Proteins Involved in the Development of Diabetes. *Molecules*, 26(19), 1–23. <https://doi.org/10.1002/0471141755.ph0912s49>
4. Aware, C. B., Patil, D. N., Suryawanshi, S. S., Mali, P. R., Rane, M. R., Gurav, R. G., & Jadhav, J. P. (2022). Natural bioactive products as promising therapeutics: A review of natural product-based drug development. *South African Journal of Botany*, 151, 512–528. <https://doi.org/10.1016/j.sajb.2022.05.028>
5. Banerjee, P., Kemmler, E., Dunkel, M., & Preissner, R. (2024). ProTox 3.0: A webserver for the prediction of toxicity of chemicals. *Nucleic Acids Research*, 52, 513–520. <https://doi.org/10.1093/nar/gkae303>
6. Chaudhary Kurmi, S. P., & Karati, D. (2025). Inhibitory potential of polyphenolic stilbene derivatives with Glycogen Synthase Kinase-3 $\beta$  (GSK-3 $\beta$ ) for Alzheimer's disease: Computational and SAR insights. *Brain Disorders*, 17, 100182. <https://doi.org/10.1016/j.dscb.2025.100182>
7. Chen, S., Mu, Z., Yong, T., Gu, J., & Zhang, Y. (2022). Grifolamine A, a novel bis- $\gamma$ -butyrolactone from *Grifola frondosa* exerted inhibitory effect on  $\alpha$ -glucosidase and their binding interaction: Affinity and molecular dynamics simulation. *Current Research in Food Science*, 5, 2045–2052. <https://doi.org/10.1016/j.crfs.2022.10.026>
8. Deogratias, G., Shadrack, D. M., Munissi, J. J. E., Kinunda, G. A., Jacob, F. R., Mtei, R. P., Masalu, R. J., Mwakyula, I., Kiruri, L. W., & Nyandoro, S. S. (2022). Hydrophobic  $\pi$ - $\pi$  stacking interactions and hydrogen bonds drive self-aggregation of luteolin in water. *Journal of Molecular Graphics and Modelling*, 116, 1010. <https://doi.org/10.1016/j.jmgm.2022.108243>
9. Dewijanti, I., MANGUNWARDYO, W., ASTARI DWIRANTI, MUHAMMAD HANAFI, & NINA ARTANTI. (2020). Short communication: Effects of the various source areas of Indonesian bay leaves (*Syzygium polyanthum*) on chemical content and antidiabetic activity. *Biodiversitas Journal of Biological Diversity*, 21(3), 1190–1195. <https://doi.org/10.13057/biodiv/d210345>
10. Džidić-Krivić, A., Sher, E. K., Kusturica, J., Farhat, E. K., Nawaz, A., & Sher, F.

- (2024). Unveiling drug induced nephrotoxicity using novel biomarkers and cutting-edge preventive strategies. *Chemico-Biological Interactions*, 388, 1–16. <https://doi.org/10.1016/j.cbi.2023.110838>
11. Gharge, S., Khagawad, P., Palled, M. S., Maste, M. M., & Suryawanshi, S. S. (2021). In-Silico Molecular Docking in Screening of Anti-Diabetic Therapeutics from Medicinal Plants. *International Journal of Ayurvedic Medicine*, 12(2), 190–198. <https://doi.org/10.30574/wjbphs.2025.23.2.0755>
  12. IDF. (2025). *IDF Diabetes Atlas 11th Edition*. <https://pubmed.ncbi.nlm.nih.gov/40874767/>
  13. Irannejad, H., Emami, S., Mirzaei, H., & Hashemi, S. M. (2020). Data on molecular docking of tautomers and enantiomers of ATTAF-1 and ATTAF-2 selectivity to the human/fungal lanosterol-14  $\alpha$ -demethylase. *Data in Brief*, 31, 1–10. <https://doi.org/10.1016/j.dib.2020.105942>
  14. Irham, L. M., Adikusuma, W., Illian, D. N., Mazaya, M., Mubaraq, A., Ma'ruf, M., Rizki, N. K., Mutia, M. S., Ali, H. M., & Basyuni, M. (2025). Deciphering anti-colorectal cancer potential of *Avicennia alba* bioactives via network pharmacology and in vitro validation. *Scientific Reports*, 1–19. <https://doi.org/10.1038/s41598-025-12500-x>
  15. Ismail, A., & Wan Ahmad, W. A. N. (2019). *Syzygium polyanthum* (Wight) Walp: A potential phytomedicine. *Pharmacognosy Journal*, 11(2), 429–438. <http://doi.org/10.5530/pj.2019.11.67>
  16. Jeyaraj, E. J., Lim, Y. Y., & Choo, W. S. (2021). Extraction methods of butterfly pea (*Clitoria ternatea*) flower and biological activities of its phytochemicals. *Journal of Food Science and Technology*, 58(6), 2054–2067. <https://doi.org/10.1007/s13197-020-04745-3>
  17. Khan, T., Lawrence, A. J., Azad, I., Raza, S., & Khan, A. R. (2018). Molecular Docking Simulation with Special Reference to Flexible Docking Approach. *JSM Chem*, 6, 1053. <https://doi.org/10.47739/2334-1831/1053>
  18. Kus, M., Ibragimow, I., & Piotrowska-Kempisty, H. (2023). Caco-2 Cell Line Standardization with Pharmaceutical Requirements and In Vitro Model Suitability for Permeability Assays. *Pharmaceutics*, 15(11). <https://doi.org/10.3390/pharmaceutics15112523>
  19. Kusuma, J., Analiasari, Wahyudi, A., Abdullah, M. K., Hasan, A. Z., Asrowardi, I., Fitriani, & Tahir, M. (2025). Diversity of the non-targeted metabolomic data across various varieties of Cloves (*Syzygium* spp.). *Data in Brief*, 58, 111237. <https://doi.org/10.1016/j.dib.2024.111237>
  20. Kwiatkowska, E., Domański, L., Dziejewski, V., Kajdy, A., Stefańska, K., & Kwiatkowski, S. (2021). The mechanism of drug nephrotoxicity and the methods for preventing kidney damage. *International Journal of Molecular Sciences*, 22(11). <https://doi.org/10.3390/ijms22116109>
  21. Liu, L., Barber, E., Kellow, N. J., & Williamson, G. (2025). Improving quercetin bioavailability: A systematic review and meta-analysis of human intervention studies. *Food Chemistry*, 477, 1–21. <https://doi.org/10.1016/j.foodchem.2025.143630>

22. Ma, S., McGann, M., & Enyedy, I. J. (2021). The influence of calculated physicochemical properties of compounds on their ADMET profiles. *Bioorganic and Medicinal Chemistry Letters*, 36(December 2020), 127825. <https://doi.org/10.1016/j.bmcl.2021.127825>
23. Mahmoud Dogara, A. (2021). Review of Ethnopharmacology, Morpho-Anatomy, Biological Evaluation and Chemical Composition of *Syzygium polyanthum* (Wight) Walp. *Plant Science Today*, 9(1), 167–177. <https://doi.org/10.14719/pst.1386>
24. Moaberfard, Z. F. (2019). Ethnopharmacological studies on anti-diabetic medicinal plants. *International Journal of Pharmacy and Pharmaceutical Science*, 1(2), 34–37. <https://doi.org/10.33545/26647222.2019.v1.i2a.96>
25. Nizamuddin, N. D., Roopa, D., Pramodini, A., Shams, S. A., Achari, P. V. K., & Reddy, K. S. (2024). In – Silico Biological Evaluation of Anticancer Drugs - SWISS ADME. *FUTURE JOURNAL OF PHARMACEUTICALS AND HEALTH SCIENCES*, 4, 86–95. <https://doi.org/10.26452/fjphs.v4i2.604>
26. Noorlander, A., Wesseling, S., Rietjens, I. M. C. M., & van Ravenzwaay, B. (2023). Predicting acute paraquat toxicity using physiologically based kinetic modelling incorporating in vitro active renal excretion via the OCT2 transporter. *Toxicology Letters*, 388, 30–39. <https://doi.org/10.1016/j.toxlet.2023.10.001>
27. Ojuka, P., Kimani, N. M., Apollo, S., Nyariki, J., Ramos, R. S., & Santos, C. B. R. (2023). Phytochemistry of the *Vepris* genus plants: A review and in silico analysis of their ADMET properties. *South African Journal of Botany*, 157, 106–114. <https://doi.org/10.1016/j.sajb.2023.03.057>
28. Olaokun, O. O., & Zubair, M. S. (2023). Antidiabetic Activity, Molecular Docking, and ADMET Properties of Compounds Isolated from Bioactive Ethyl Acetate Fraction of *Ficus lutea* Leaf Extract. *Molecules*, 28(23), 1–19. <https://doi.org/10.3390/molecules28237717>
29. Parisa, N., Tamzil, N. S., Handayati Harahap, D., Dwi Prasasty, G., Hidayat, R., Maritska, Z., & Prananjaya, B. A. (2019). The effect of Leaf Salam Extracts (*Syzygium polyanthum*) in diabetes mellitus therapy on wistar albino rats. *Journal of Physics: Conference Series*, 1246(1). <https://doi.org/10.1088/1742-6596/1246/1/012034>
30. Pirintsos, S., Panagiotopoulos, A., Bariotakis, M., Daskalakis, V., Lionis, C., Sourvinos, G., Karakasiliotis, I., Kampa, M., & Castanas, E. (2022). From Traditional Ethnopharmacology to Modern Natural Drug Discovery: A Methodology Discussion and Specific Examples. *Molecules*, 27(13), 1–18. <https://doi.org/10.3390/molecules27134060>
31. Pollastri, M. P. (2010). Overview on the rule of five. *Current Protocols in Pharmacology*, SUPPL. 49, 1–8. <https://doi.org/10.1002/0471141755.ph0912s49>
32. Quinlan, M. B. (2022). Ethnomedicines. In *A Companion to Medical Anthropology* (Issue March, pp. 315–341). Wiley. <https://doi.org/10.1002/9781119718963.ch18>
33. Rahim, E. N. A. A., Ismail, A., Omar, M. N., Rahmat, U. N., & Nizam Wan Ahmad, W. A. (2018). GC-MS analysis of phytochemical compounds in *syzygium polyanthum* leaves extracted using ultrasound-assisted method. *Pharmacognosy*

- Journal*, 10(1), 110–119. <http://dx.doi.org/10.5530/pj.2018.1.20>
34. Renzo, L. Di, Gualtieri, P., & De Lorenzo, A. (2021). Diet, Nutrition and Chronic Degenerative Diseases. *Nutrients*, 13(4), 1. <https://doi.org/10.3390/nu13041372>
35. Reza, S. M., Qiu, C., Lin, X., Su, K.-J., Liu, A., Zhang, X., Gong, Y., Luo, Z., Tian, Q., Nwadiugwu, M., Liang, S., Shen, H., & Deng, H.-W. (2025). An Attention- -Aware Multi- - Task Learning Framework Identifies Candidate Targets for Drug Repurposing in Sarcopenia. *Journal of Cachexia, Sarcopenia and Muscle ORIGINAL*, 1–12. <https://doi.org/10.1002/jcsm.13661>
36. Rhabori, S. El, El Allouche, Y., Naanaai, L., El Aissouq, A., Khalil, F., Alaqarbeh, M., Bouachrine, M., & Chtita, S. (2025). Exploring innovative strategies for identifying anti-breast cancer compounds by integrating 2D/3D-QSAR, molecular docking analyses, ADMET predictions, molecular dynamics simulations, and MM-PBSA approaches. *Journal of Molecular Structure*, 1320(July 2024), 1–18. <https://doi.org/10.1016/j.molstruc.2024.139500>
37. Rinaldi, S., Colombo, G., & Paladino, A. (2022). The dynamics of t1 adenosine binding on human Argonaute 2 : Understanding recognition with conformational selection. *The Protein Society*, 1–12. <https://doi.org/10.1002/pro.4377>
38. Sanober, A., & Agarwal, N. (2021). Quantitative Structure-Activity Relationship and Molecular Modeling Studies on a Series of Hydroxypyrrolo[2,1-c][1,4]Benzodiazepine-5,11-dione Acting as Angiotensin Converting Enzyme I Inhibitors. *Der Pharma Chemica*, 13(2), 11–26. <https://www.derpharmachemica.com/pharma-chemica/quantitative-structureactivity-relationship-and-molecular-modeling-studies-on-a-series-of-hydroxypyrrolo21c14benzodiazepine511dion-64303.html>.
39. Silva, D. V. S. P. da, Nascimento, P. H. do B., Rocha, J. V. R. da, Marques, D. S. C., Brayner, F. A., Alves, L. C., Araújo, H. D. A. de, Cruz Filho, I. J. da, Albuquerque, M. C. P. de A., Lima, M. do C. A. de, & Aires, A. de L. (2023). In vitro activity, ultrastructural analysis and in silico pharmacokinetic properties (ADMET) of thiazole compounds against adult worms of *Schistosoma mansoni*. *Acta Tropica*, 245(April). <https://doi.org/10.1016/j.actatropica.2023.106965>
40. Thi, L., Quyen, T., & Trung, N. T. (2024). Noticeable characteristics of conventional and nonconventional hydrogen bonds in the binary systems of chalcogenoaldehyde and chalcogenocarboxylic acid derivatives. *Royal Society of Chemistry*, 14, 1–13. <https://doi.org/10.1039/d4ra07498j>
41. Tseng, T.-S., Lin, W.-T., Gonzalez, G. V, Kao, Y.-H., Chen, L.-S., & Lin, H.-Y. (2021). Sugar intake from sweetened beverages and diabetes: A narrative review. *World Journal of Diabetes*, 12(9), 1530–1538. <https://doi.org/10.4239/wjd.v12.i9.1530>
42. Venkanna, A., Subedi, L., Teli, M. K., Lama, P. D., Nangunuri, B. G., Lee, S.-Y., Kim, S. Y., & Kim, M.-H. (2020). Positioning of an unprecedented spiro [ 5 . 5 ] undeca ring system into kinase inhibitor space. *Scientific Reports*, 1–17. <https://doi.org/10.1038/s41598-020-78158-9>
43. Verma, A., Shukla, S., Gupta, P., Kumar, S., Singh, R. P., Banerjee, M., Bishnoi, A., Sarkar, J., Sethi, A., & Singh, S. K. (2025). Assessment of anti-cancer activity, DFT,

- molecular docking, thermodynamic properties and ADMET studies of novel steroidal derivatives containing aceclofenac moiety. *Journal of Molecular Structure*, 1340(April), 142530. <https://doi.org/10.1016/j.molstruc.2025.142530>
44. Welz, A. N., Emberger-Klein, A., & Menrad, K. (2018). Why people use herbal medicine: Insights from a focus-group study in Germany. *BMC Complementary and Alternative Medicine*, 18(1), 1–9. <https://doi.org/10.1186/s12906-018-2160-6>
45. Widodo, A., Sulastri, E., Ihwan, I., Cahyadi, M. H., Maulana, S., & Zubair, M. S. (2024). Antidiabetic Activity, Phytochemical Analysis, and Acute Oral Toxicity Test of Combined Ethanolic Extract of *Syzygium polyanthum* and *Muntingia calabura* Leaves. *Scientific World Journal*, 2024. <https://doi.org/10.1155/2024/3607396>
46. Widyawati, T., Syahputra, R. A., Syarifah, S., & Sumantri, I. B. (2023). Analysis of Antidiabetic Activity of Squalene via In Silico and In Vivo Assay. *Molecules*, 28(9), 1–14. <https://doi.org/10.3390/molecules28093783>
47. Widyawati, T., Yusoff, N. A., Bello, I., Asmawi, M. Z., & Ahmad, M. (2022). Bioactivity-Guided Fractionation and Identification of Antidiabetic Compound of *Syzygium polyanthum* (Wight.)'s Leaf Extract in Streptozotocin-Induced Diabetic Rat Model. *Molecules*, 27(20). <https://doi.org/10.3390/molecules27206814>
48. Windarsih, A., Suratno, Warmiko, H. D., Indrianingsih, A. W., Rohman, A., & Ulumuddin, Y. I. (2022). Untargeted metabolomics and proteomics approach using liquid chromatography-Orbitrap high resolution mass spectrometry to detect pork adulteration in *Pangasius hypophthalmus* meat. *Food Chemistry*, 386, 132856. <https://doi.org/10.1016/j.foodchem.2022.132856>
49. Xie, X., Wu, C., Hao, Y., Wang, T., Yang, Y., Cai, P., Zhang, Y., Huang, J., Deng, K., Yan, D., & Lin, H. (2023). Benefits and risks of drug combination therapy for diabetes mellitus and its complications: a comprehensive review. *Frontiers in Endocrinology*, 14(December), 1–17. <https://doi.org/10.3389/fendo.2023.1301093>
50. Zhao, M., Ma, J., Li, M., Zhang, Y., Jiang, B., Zhao, X., Huai, C., Shen, L., Zhang, N., He, L., & Qin, S. (2021). Cytochrome p450 enzymes and drug metabolism in humans. *International Journal of Molecular Sciences*, 22(23), 1–16. <https://doi.org/10.3390/ijms222312808>
51. Zheng, L., Cao, J., Jing, L., Kang, D., Wang, Z., & Liu, X. (2025). Convergence of Computer-Aided Drug Discovery and Artificial Intelligence: Towards Next-Generation Therapeutics. *Pharmaceutical Science Advances*, 4, 1–15. <https://doi.org/10.1016/j.pscia.2025.100100>